THERMOMECANICAL ANALYSIS OF THE PURE TANTALUM DEFORMED VIA THE EQUAL CHANNEL ANGULAR PRESSING

Fabiane Roberta Freitas da Silva, fabiane@metal.eeimvr.uff.br
Neil de Medeiros, neil@metal.eeimvr.uff.br
Luciano Pessanha Moreira, luciano.moreira@metal.eeimvr.uff.br
Jefferson Fabrício Cardoso Lins, jfclins@metal.eeimvr.uff.br
Jayme Pereira de Gouvêa, jpg@metal.eeimvr.uff.br
Programa de Pós-graduação em Engenharia Metalúrgica, Universidade Federal Fluminense
Avenida dos Trabalhadores, 420, Volta Redonda - RJ, 27255-125, Brazil.

Abstract. *In the present work, an adiabatic thermomecanical idealization to metallic materials deformed after a single pass at room temperature of equal channel angular pressing, combined to the pressing load prediction calculated with the upper-bound solutions proposed by Pérez e Luri [Mech. Mater. 40 (2008) 617] is proposed. Also, a plane-strain finite-element model is constructed to provide the load, effective plastic strain and workpiece temperature curves in function of the punch displacement. For the theoretical and numerical analyses, a die with channels intersected at 90º and an outer fillet radius of 5 mm was considered and an ideal lubrication condition was assumed. Regarding the thermomecanical properties of the pure tantalum adjusted to the Johnson-Cook hardening law and employing the isotropic plasticity criterion of von Mises, the numerical results of pressing load showed that during the passage of the billet bottom portion forward the die exit channel, the load considerably increases and, then, it falls down continuously for a constant velocity value. Also, it was possible to verify the elevation of the billet temperature associated to the rising of effective plastic strain during the pressing. The theoretical analyses consistently showed the exponential increasing of the pressing force and the sample temperature when the velocity was magnified to 100 times, due to the high strain-rate sensitivity of the employed material. Finally, by comparing the numerical and theoretical predictions of load, effective plastic strain and temperature, the proposed adiabatic solutions could be validated.*

Keywords*: Equal channel angular pressing, finite-element method, upper-bound method, thermomechanical behavior, pure tantalum.*

1. INTRODUCTION

Aiming to meet the increasing demand for materials with superior properties for application in the metalworking industry, various metal forming processes are applied. These processes aim to change the microstructure of metals by reducing the grain size. However, in conventional processes such as rolling, for example, when the strength of certain materials rises, there is a loss or deterioration of other properties such as ductility. To avoid this deficiency, unconventional deformation methods based on severe plastic deformation (SPD) have been developed aiming to achieve a microstructure composed of ultrafine and/or nanocrystalline grains possessing large fraction of high angle boundaries, and as a result, high mechanical properties of metals.

Among the techniques developed, equal channel angular pressing (ECAP) is one of the most attractive. In this technique a billet is forced to flow through a die that contains two channels of identical cross section and intercept each other at an angle of Φ, which can range between 90º and 150º (Segal, 1995). Also according to Segal (1995), while passing through the intersection zone between channels, the material is deformed by simple shear. Langdon (2007) points out that the deformation imposed on billet depends on the values adopted for Φ and Ψ, which represents the curvature of material during its passage through the deformation zone, intersection between channels.

Prangnell (1997) and Kim (2002), showed that other factors such as friction and deformation routes also have great influence on the distribution of strain in the billet after deformation. However, only some works are concerned in the heat generation during ECAP. Among them, Pei et al. (2005) and Dumoulin et al. (2005) observed that its growth can affect the grain size at the end of deformation and material flow behavior. In this context, the present work is focused on the evaluation of the temperature rising during the processing of metals via ECAP technique. For that, upper-bound and finite-element models combined to Johnson-Cook, JC, work hardening law and von Mises isotropic plasticity criterion were used to analyze the adiabatic heat generation during the cold single-pass extrusion of pure tantalum initially at high speed.

2. MATERIAL AND METHODS

2.1. Material

Table 1 shows the thermo-mechanical properties for pure tantalum obtained for Liang and Khan (1999) after adjusting with the JC-model.

Table 1. Thermo-mechanical properties of pure tantalum.

Density (kg/m^3)	16,650
Specific heat (J/kg ºC)	153
Modulus of elasticity (Pa)	186000000
Poisson's ratio	0.35
Melting temperature (ºC)	2,996
Reference temperature (ºC)	25
A (Pa)	185000000
B (Pa)	675000000
C	0.047
mJC	0.425
n	0.3

2.2. Methods

2.2.1. Finite-element modeling

The pressing of a pure tantalum billet at room temperature was carried out at 10 mm / s with the help of the finite-element method by using the program ABAQUS 6.8/Explicit. In this way, plane-strain finite-element models were proposed for both tooling and sample.

In relation to the tooling, that is, the die and punch and billet were employed about 1,400 -type elements On the other hand, for the 65 mm x 10 mm x 1 mm billet modeling, the total number of CPE4R elements was close to 10,400. Also, as showed in Fig. 1, the die geometry considered in this work was composed by channels intersected at 90º and outer fillet radius about 5 mm in order to facilitate the material processing.

In terms of mechanical behaviour, both die and punch were considered as H13 steel rigid-elastic pieces by adopting the Elasticity modulus, E, equal to 210 GPa and a Poisson's ratio, ν, of 0.3.

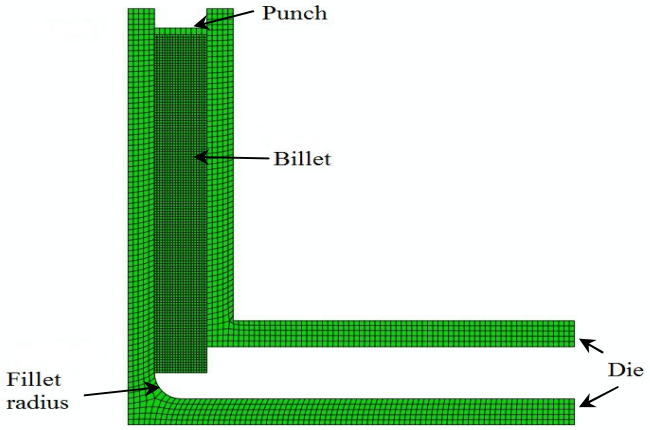

Figure 1. Schematic illustration of the ECAP finite-element modeling proposed in the present work.

2.2.2. Upper-bound formulation

In this work, the upper-bound solutions proposed by Pérez and Luri (2008) to calculate the pressing pressure for the die configurations presented in Fig. 2 were associated to the von Mises criterion. Also, from the solutions developed by Luri et al. (2006) for the effective plastic strains determination, analytical expressions to predict the total deformation time, t_D, mean yield stress, $\overline{\sigma}$, and the temperature increment, ΔT, by taking into account the relationship between thermal and mechanical materials behavior provided by the adopted adiabatic heat hypothesis.

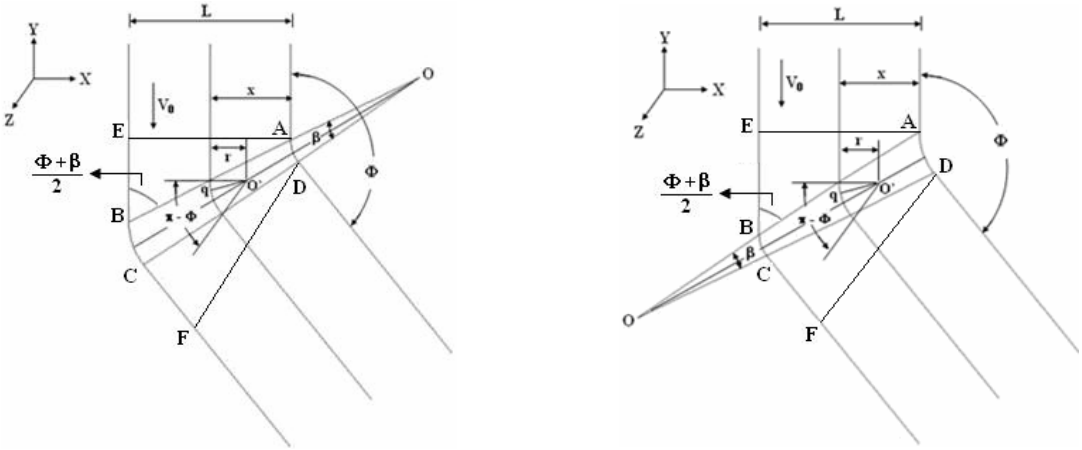

(a) (b)

Figure 2. Die geometries considered in the upper-bound modeling. (a) inner radius, R_{inner} < outer, R_{outer}, and (b) R_{inner} > R_{outer}. Adapted from Pérez and Luri (2008).

According to Pérez and Luri (2008), for the constant pressing velocity, V_0, the pressing pressure is given by:

$$p = \kappa \left\{ \frac{(\pi - \Phi)}{sin\left(\frac{\Phi+\beta}{2}\right)} + f\left[\frac{2H}{L} + (\pi - \Phi)\left(\frac{R_{inner} + R_{outer}}{L}\right)\left(1 - \frac{1}{sin\left(\frac{\Phi+\beta}{2}\right)}\right) + \frac{2H}{W} \right] \right\} \quad R_{inner} < R_{outer}$$

$$p = \kappa \left\{ \frac{(\pi - \Phi)}{sin\left(\frac{\Phi-\beta}{2}\right)} + f\left[\frac{2H}{L} + (\pi - \Phi)\left(\frac{R_{inner} + R_{outer}}{L}\right)\left(1 - \frac{1}{sin\left(\frac{\Phi-\beta}{2}\right)}\right) + \frac{2H}{W} \right] \right\} \quad R_{inner} > R_{outer} \tag{1}$$

where κ, Φ, f, H, L e W denote the pure shear yield stress, die channels intersection angle, Tresca friction factor, height and width of the billet, respectively. It is clear that pressing force, F, is equal to p times the billet cross-section.

The angle β related to the fillet radius is calculated by,

$$\beta = 2\,arctan\left\{ \frac{(R_{outer} - R_{inner})\,tan[\Phi/2]}{L + (R_{inner} - R_{outer}) + L\,tan^2[\Phi/2]} \right\} \quad \rightarrow R_{inner} < R_{outer}$$

$$\beta = 2\,arctan\left\{ \frac{(R_{inner} - R_{outer})\,tan[\Phi/2]}{L + (R_{inner} - R_{outer}) + L\,tan^2[\Phi/2]} \right\} \quad \rightarrow R_{inner} > R_{outer} \tag{2}$$

In relation to material yielding, the plasticity condition establish that,

$$f(\sigma_{ij}, \bar{\varepsilon}^p, \dot{\bar{\varepsilon}}^p, T) = F(\sigma_{ij}) - \bar{\sigma}(\bar{\varepsilon}^p, \dot{\bar{\varepsilon}}^p, T) = 0 \tag{3}$$

where f defines the yielding function, F (σ_{ij}) is the von Mises criterion associated to the yielding surface size and $\bar{\sigma}$ depends on the scalar measures of effective plastic strain, $\bar{\varepsilon}^p$, and strain-rate, $\dot{\bar{\varepsilon}}^p$.

The isotropic von Mises plasticity criterion is well-known defined in terms of the second invariant, J_2 of the Cauchy stress tensor, σ_{ij}, deviatoric component, that is, the tensor S_{ij}. Therefore, it is also called J_2 criterion and it is defined as,

$$F(\sigma_{ij}) = \sqrt{\frac{3}{2} S_{ij} S_{ij}} \tag{4}$$

The ECAP associated simple shear stress state is correctly identified as pure shear plus rigid motion. Thus, by using the J_2 criterion, the in-plane pure shear ($S_{12} = S_{21} = \kappa$; others $S_{ij} = 0$) for the plasticity condition defined in Eq. (3) is given by,

$$\kappa = \frac{\bar{\sigma}}{\sqrt{3}} \tag{5}$$

where κ denotes the pure shear yield stress.

The Cauchy infinitesimal plastic strain tensor components were determined under the isotropic work-hardening hypothesis. In this way, the associated flow rule postulated that,

$$\dot{\varepsilon}_{ij}^{\,p} = \dot{\lambda}\frac{\partial f}{\partial \sigma_{ij}} = \dot{\lambda}\frac{\partial F(\sigma_{ij})}{\partial \sigma_{ij}} \tag{6}$$

where $\dot{\lambda}$ is the plastic multiplier or plastic modulus and $\dot{\varepsilon}_{ij}^{\,p}$ denotes the plastic strain-rate tensor. By combining the Euler's identity to the plastic work equivalency principle, one can verify that $\dot{\lambda} = \dot{\bar{\varepsilon}}^{\,p}$. Therefore, by squaring both sides of the Eq. (6), the effective plastic strain-rate can be obtained in terms of the von Mises criterion. Thus,

$$\dot{\bar{\varepsilon}}^{\,p} = \sqrt{\frac{2}{3}\dot{\varepsilon}_{ij}^{\,p}\,\dot{\varepsilon}_{ij}^{\,p}} \tag{7}$$

where $\dot{\bar{\varepsilon}}^{\,p}$ defines the effective plastic strain-rate. Here, we consider the effective plastic strain as an accumulated measure after the pressing process. For that reason, this scalar parameter is calculated by integrating the Eq. (7) from zero to total deformation time, t_D, that the material undergoes severe plastic forming. Consequently,

$$\bar{\varepsilon}^{\,p} = \int_{t_0=0}^{t_D} \sqrt{\frac{2}{3}\,\dot{\varepsilon}_{ij}^{\,p}\,\dot{\varepsilon}_{ij}^{\,p}}\; dt \tag{8}$$

And according to Fig. (2), the time t_D is obtained in the form,

$$\begin{aligned} t_D &= \frac{L}{V_0}\left\{2\,cotan\left(\frac{\Phi+\beta}{2}\right) + \frac{(\pi-\Phi)}{L}\left(1-cotan\left(\frac{\Phi+\beta}{2}\right)tan\left(\frac{\Phi}{2}\right)\right)\left[R_{inner} + L\left(1-cotan\left(\frac{\Phi+\beta}{2}\right)tan\left(\frac{\Phi}{2}\right)\right)\right]\right\} \quad R_{inner} < R_{outer} \\ t_D &= \frac{L}{V_0}\left\{2\,cotan\left(\frac{\Phi-\beta}{2}\right) + \frac{(\pi-\Phi)}{L}\left(1-cotan\left(\frac{\Phi-\beta}{2}\right)tan\left(\frac{\Phi}{2}\right)\right)\left[R_{inner} + L\left(1-cotan\left(\frac{\Phi-\beta}{2}\right)tan\left(\frac{\Phi}{2}\right)\right)\right]\right\} \quad R_{inner} > R_{outer} \end{aligned} \tag{9}$$

where L and V_0 denote the billet total height and the initial pressing velocity, respectively.

Considering the pure shear in terms of plastic strain-rate, in which $2\,\dot{\varepsilon}_{ij}^{\,p} = \dot{\gamma}^{\,p}$, associated to plastic shear strain-rate $\dot{\gamma}^{\,p} = (\gamma^p / t_D)$, we have

$$\bar{\varepsilon}^{\,p} = \frac{1}{\sqrt{3}}\,\gamma^p \tag{10}$$

And to express the plastic shear strain, γ^p, Luri et al. (2006) proposed the following equations:

$$\begin{aligned} \gamma^p &= 2cotan\left(\frac{\Phi+\beta}{2}\right) + (\pi-\Phi)\left[1-cotan\left(\frac{\Phi+\beta}{2}\right)tan\left(\frac{\Phi}{2}\right)\right] \quad \rightarrow R_{inner} < R_{outer} \\ \gamma^p &= 2\,cotan\left(\frac{\Phi-\beta}{2}\right) + (\pi-\Phi)\left[1-cotan\left(\frac{\Phi-\beta}{2}\right)tan\left(\frac{\Phi}{2}\right)\right] \quad \rightarrow R_{inner} > R_{outer} \end{aligned} \tag{11}$$

In the present work, the coupling between plastic and thermal behaviors is modeled through the adiabatic heat equation that relates the temperature increment and the product between the effective plastic stress and strain. Thus,

$$\Delta T = \frac{\eta}{\rho c_p} \bar{\sigma}\, \bar{\varepsilon}^p \tag{12}$$

where η, ρ and c_p denote the Taylor-Quinney factor (equal to 0.9) and the material density and specific heat, respectively.

The equivalent stress is identified in terms of its mean value that is associated to the integration of the JC-model for the accumulated effective plastic strain, that is,

$$\bar{\sigma} = AC\left\{\left[1-\left(\frac{T_f - T_{ref}}{T_{fus} - T_{ref}}\right)^{mJC}\right]\left[\frac{1}{C}+ln\left(\frac{\bar{\varepsilon}^p}{t_D}\right)-1\right]\right\}+BC\left\{\left[\frac{(\bar{\varepsilon}^p)^n}{(n+1)}\left(1-\left(\frac{T_f - T_{ref}}{T_{fus} - T_{ref}}\right)^{mJC}\right)\right]\left[\frac{1}{C}+ln\left(\frac{\bar{\varepsilon}^p}{t_D}\right)-\frac{1}{(n+1)}\right]\right\} \tag{13}$$

where T_f, T_{ref} and T_{fus} represent the final, reference and melting temperatures. The values of each parameters of Eq (13) are listed on Tab. 1. Returning (13) into (12), the temperature increment is nonlinearly calculated by,

$$\begin{aligned}&\Delta T + \frac{\beta_T}{\rho c_p}\left\{AC\,\bar{\varepsilon}^p\left[\left(\frac{T_f - T_{ref}}{T_{fus} - T_{ref}}\right)^{mJC}\left(\frac{1}{C}+ln\left(\frac{\bar{\varepsilon}^p}{t_D}\right)-1\right)\right]+\frac{BC(\bar{\varepsilon}^p)^{n+1}}{(n+1)}\left[\left(\frac{T_f - T_{ref}}{T_{fus} - T_{ref}}\right)^{mJC}\left(\frac{1}{C}+ln\left(\frac{\bar{\varepsilon}^p}{t_D}\right)-\frac{1}{(n+1)}\right)\right]\right\} = \\ &= \frac{\beta_T}{\rho c_p}\left\{AC\,\bar{\varepsilon}^p\left(\frac{1}{C}+ln\left(\frac{\bar{\varepsilon}^p}{t_D}\right)-1\right)+\frac{BC(\bar{\varepsilon}^p)^{n+1}}{(n+1)}\left(\frac{1}{C}+ln\left(\frac{\bar{\varepsilon}^p}{t_D}\right)-\frac{1}{(n+1)}\right)\right\}\end{aligned} \tag{14}$$

And the final temperature due the heating promoted on the material by the plastic work is given by,

$$T_f = T_{ini} + \Delta T \tag{15}$$

where T_{ini} denotes the initial temperature that the sample was placed into the ECAP die. As we are modeling the cold pressing of the billets, it is intuitive that T_{ini} = 25ºC. Also, due to nonlinear character of Eq. (14), it is numerically solved with the help of the bisection method.

The conditions of the analyses performed in the present work, i.e., billet dimensions, die geometrical parameters, tribology and pressing velocities are listed on Tab. 2.

Table 2. Parameters considered in the theoretical and numerical analyses.

Parameter	FEM simulation	Upper-bound evaluation
L (mm)	10	10
H (mm)	65	65
Φ (degree)	90	90
R_{inner} (mm)	0	0
R_{outer} (mm)	5	5
Friction factor, f	-	0.10
Friction coefficient, μ	0.05 (~ f / √3)	-
V_0 (mm / s)	10	0.1 - 10

Finally, after the individual numerical and analytical evaluations, the proposed upper-bound model with thermal coupling was validated from the comparison with the FEM maximum predictions of pressing pressure, temperature and effective plastic strain.

3. RESULTS AND DISCUSSION

3.1 Finite-element results

Figure 3 presents the results of pressing force, sample temperature and effective plastic strain for the pure tantalum deformed after one pass of ECAP from the adiabatic plane strain finite element modelling. A global evaluation of the obtained predictions permits to note the direct relationship between the progressive material deformation process, represented by the billet displacement, and the continuous increasing of the imposed effective plastic strains and the sample temperature. In fact, the billet straining rises during the pressing and, consequently, the realized plastic work promotes it associated heating.

In relation to the pressing force, Fig. 3(a), one can firstly observe the maximum value of 117 kN close to 5 mm of the punch displacement and a subsequent decreasing of load after 10 mm. As previously reported by Altan and co-workers (2005), this aspect can be explained by the passage of billet bottom portion forward the exit channel that causes a considerable elevation of the needed load. As it follows, the deformation process becomes lesser severe and, for that, a continuous drop of the required force is observed until the end of the pressing, in the present case, after 60 mm of displacement.

The aspects related to the results of effective plastic strain and the billet temperature in function of the punch motion are depicted on Figs. 3 (b) and (c), respectively. Although the pressing force falls down after 10 mm of displacement, due to the maximum considered effective plastic strain value of 1.16 in the work-hardening curve introduced into the finite-element model, the workpiece plastic deformation process continuously induces permanent strain along its surface. However, for the high dependency of the effective plastic strain with the die geometry, the presence of the outer fillet radius reduces it maximum level to 0.80 and provides the respective also maximum billet temperature of 205ºC numerically obtained by using the Eq. (12).

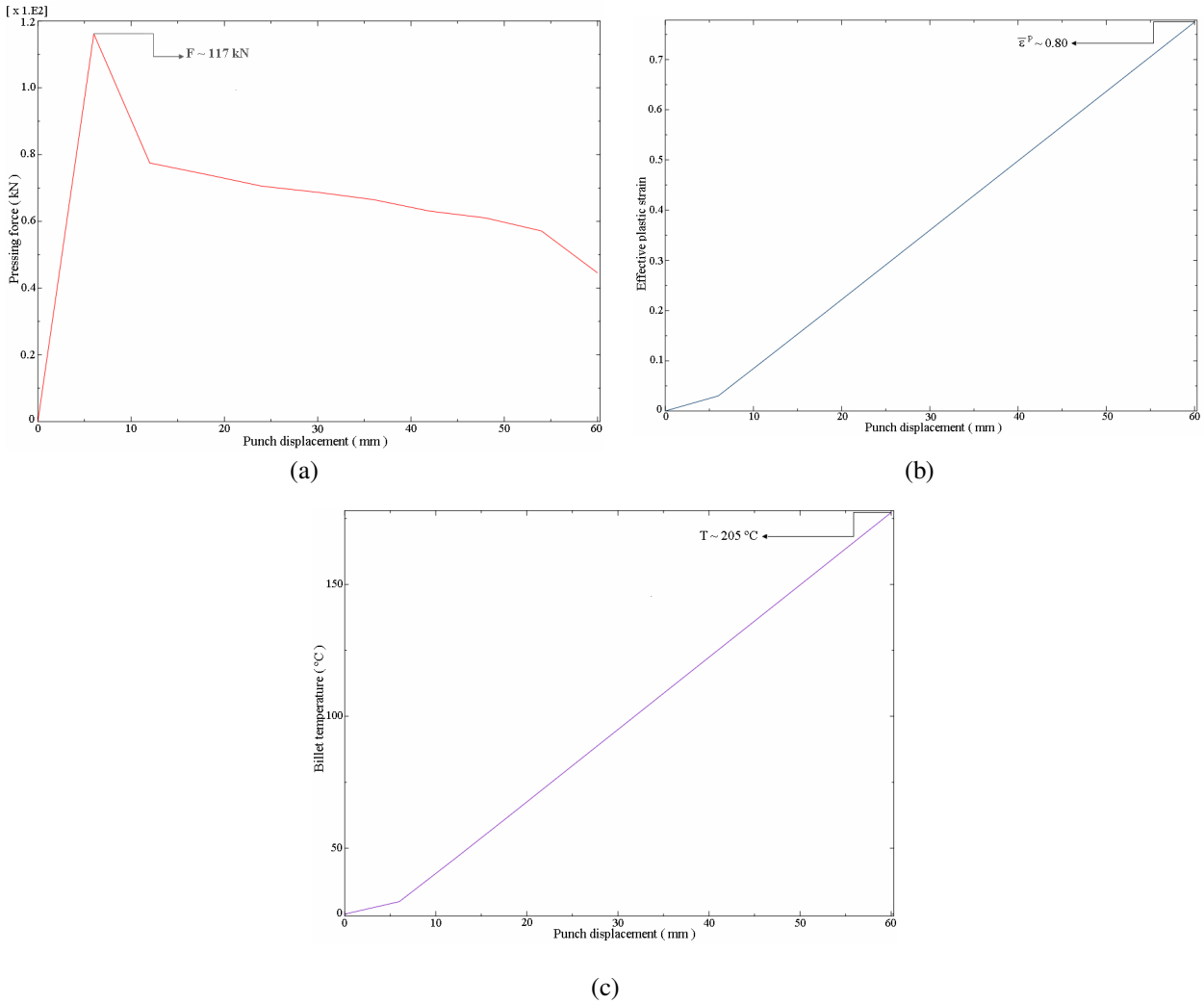

Figure 3. Results obtained with the adiabatic plane-strain finite-element model in function of the billet displacement. (a) pressing force; (b) effective plastic strain and (c) billet final temperature.

The direct coupling between the effective plastic strain and the sample temperature can be verified for the iso-contours of finite-element nodal results presented in Fig. 4. Beyond the similarity between the distributions of effective plastic strains and temperature, it is noticeable that the yellow regions define both the effective plastic strain and thermal homogeneous zone and, according to observations of Pei et al. (2005) for the pure aluminium, it is responsible to the superior mechanical strength of the deformed metallic materials. Therefore, for the proposed adiabatic heat generation modelling, one can testify that the plastic work plays a primary role in the sample temperature changing when a ideal lubrication condition is assumed.

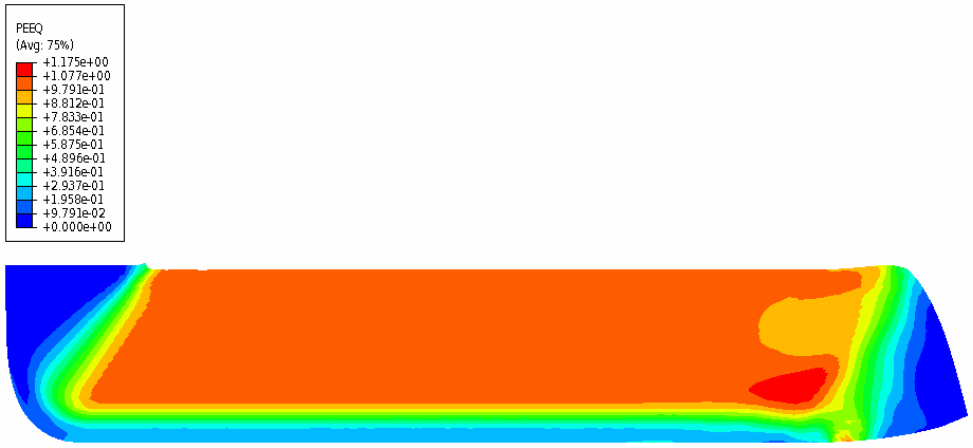

(a)

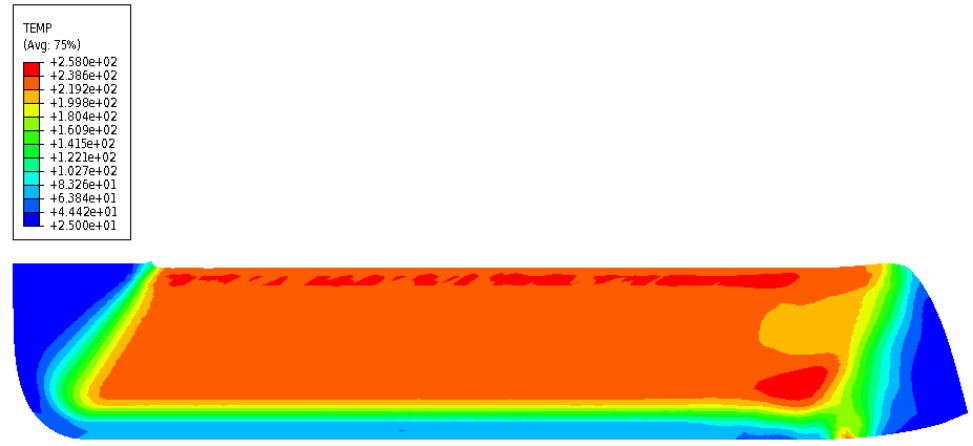

(b)

Figure 4. Iso-contour predictions obtained from the finite element model. (a) effective plastic strain and (b) sample temperature.

3.2 Upper-bound predictions

Figure 5 shows the pressing velocity effect on the pressing force and the pure tantalum billet temperature that are associated to the realized plastic work during the material processing into a die with $\Phi = 90^{\circ}$ and containing an outer fillet radius of 5 mm, in conditions of ideal lubrication. It is possible to observe that an increasing of 100 times on the velocity, that is, from 0.1 to 10 mm / s causes an elevation of 25kN in terms of the load, that is, from 97 to 122kN. In fact, higher velocities lead to more abrupt work-hardening levels attributed to the billet since the deformation time very short to the material internal stress/strain accommodation. In the same way, the rising of the temperature from 163 to 196ºC, i.e., equal to 33ºC for the considered velocity interval can be also explained in terms of the severity in the induced work-hardening on the material. Another important fact that can help the understanding of the thermomechanical response of pure tantalum deformed via ECAP technique is it non negligible high strain-rate sensitivity, represented by the C-parameter listed on Tab.1. At the same time, it is useful to mention that the positive exponential form of the temperature diagram depicted on Fig. 5b is coherent with the experimental predictions obtained by Pei et al. (2005) for the Al-1%Mg and Al-3%Mg alloys.

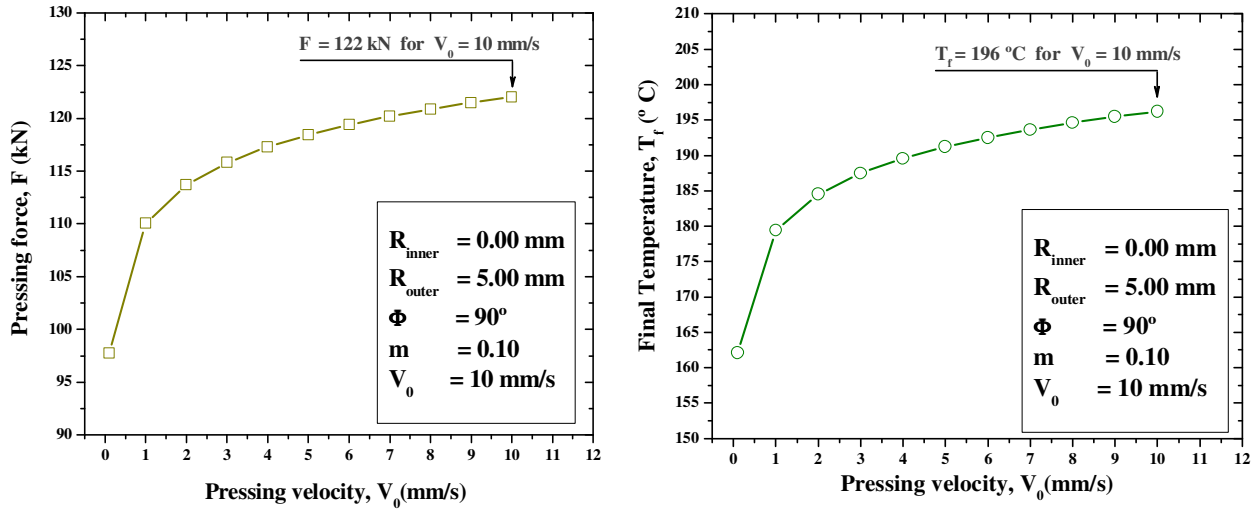

(a) (b)

Figure 5. Analytical results of pressing force and billet final temperature for distinct pressing velocity levels. (a) pressing force and (b) billet final temperature.

3.3 Validation of the non-isothermal modeling

Table 3 presents the predictions of pressing force, final temperature and effective plastic strain obtained with the both finite-element and analytical proposed models. In relation to the processing load results, it is expected a higher level in comparison to the numerical one due to conservative characteristic of the upper-bound theorem. On the other hand, the appreciable proximity between the results of the workpiece final temperature and the maximum imposed effective plastic strains is explained by the use of the Eq. (12) in the numerical and theoretical model. Thus, the theoretical model is not related to the upper-bound method and it does not provide results higher those calculated with the finite-element formulation. For these reasons, the proposed adiabatic theoretical solution to idealize the thermomechanical response of metallic materials deformed via the equal channel angular pressing technique can be validated by the confrontation with numerical results obtained from the performed plane-strain finite-element analysis.

Table 3. Comparison between FE and upper-bound results for pure tantalum deformed via ECAP.

Parameter	Results	
	FEM	Analytical model
Pressing force (kN)	117	122
Effective plastic strain	0.80	1.03
Final temperature (ºC)	205	196

4. CONCLUSIONS

An analytical thermomecanical idealization of metallic materials deformed via the equal channel angular pressing technique, after a single pass at room temperature, is proposed by using the adiabatic heat equation associated to the mean equivalent measure of stress calculated with the Johnson-Cook work-hardening law and the effective plastic strain provided by the tooling-geometry dependent solutions proposed by Luri et al. (2006). Also, the plastic material behaviour is modeled by using the isotropic criterion of von Mises and the pressing load is calculated with the upper-bound expressions recently developed by Pérez and Luri (2008). At the same time, a plane strain finite element model is constructed to simulate the pressing of metals after a single pass at room temperature. For these theoretical and numerical models, for a ideal lubrication condition, a die with channels intersected at $\Phi = 90^{\circ}$ and composed by an outer fillet radius of 5 mm was considered and the pressing velocity was assumed equal to 10 mm / s in the case of the simulations and it was varied out from 0.1 to 10 mm / s for the analytical analyses. Thus, by adopting the thermal and mechanical properties of the pure tantalum, it was possible to evaluate the sample temperature rising due to the realized plastic work and some conclusive aspects can be outlined:

1) Assuming the ideal lubrication case, the finite element developed model provided a clear observation of the temperature distribution along the billet surface and, in fact, it continuously increases with the effective plastic strain during the pressing. For the pure tantalum, the maximum pressing load about 117kN was attained after 5 mm of the punch displacement and it is associated to the sample bottom part in direction to the exit die channel. Also, the initial temperature of 25º C was elevated to 205ºC that demonstrates the intensive plastic work that is imposed on workpiece;

2) The analytical tests performed with the proposed adiabatic model permitted to verify the influence of the pressing velocity on both the load and the billet temperature. It was observed that, when the velocity is augmented in 100 times, i.e., from 0.1 to 10 mm / s, the needed load is amplified in 25 kN and the associated plastic work promotes an elevation close to 33ºC in the billet temperature. These aspects can be understood in terms of the considerable strain-rate sensitivity exhibited to the pure tantalum by means of the Johnson-Cook law;

3) The comparison between the results of maximum pressing load, effective plastic strain and billet temperature calculated with the finite-element model and the proposed analytical expressions permitted the validation of the adiabatic thermomecanical expressions developed to reproduce the heating of metals deformed by the equal channel angular pressing technique after a single pass and, initially, at room temperature.

5. REFERENCES

Segal, V.M., 1995, “Materials processing by simple shear”, Materials Science and Engineering A, Vol. 197, No. 2, pp. 157-164.

Langdon, T.G., 2007, “The principles of grain refinement in equal-channel angular pressing”, Materials Science and Engineering A, Vol. 462, pp. 3-11.

Prangnell, P.B., Harris, C. and Roberts, S.M., 1997, “Finite element modelling of equal channel angular extrusion”, Scripta Materialia, Vol. 37, No. 7, pp. 983-989.

Kim, H.S., 2002, “Finite element analysis of deformation behavior of metals during equal channel multi-angular pressing”, Materials Science and Engineering A, Vol. 328, No. 1-2, pp. 317-323.

Pei, Q.X., Hu, B.H. and Lu, C., 2005, “Thermo-mechanical modeling and analysis of equal channel angular pressing”, Journal of Metastable and Nanocrystalline Materials, Vol. 23, pp. 263-266.

Dumoulin, S., Roven, H.J., Werenskiold, J.C. and Valberg, H.S., 2005, “Finite element modeling of equal channel angular pressing: effect of material properties, friction and die geometry”, Materials Science and Engineering A, Vol. 410-411, pp. 248-251.

Liang, R. and Khan, A.S., 1999, “A critical review of experimental results and constitutive models for BCC and FCC metals over a wide range of strain rates and temperatures”, International Journal of Plasticity, Vol. 15, pp. 963-980.

Pérez, C.J.L. and Luri R., 2008, “Study of the ECAE process by the upper bound method considering the correct die design”, Mechanics of Materials, Vol. 40, pp. 617-628.

Luri, R., Pérez, C.J.L. and León, J., 2006, “A new configuration for equal channel angular extrusion dies”, Journal of Manufacturing Science and Engineering, Vol. 128, pp. 860-865.

Altan, B.S., Purcek, G., and Miskioglu, I., 2005, “An upper-bound analysis for equal-channel angular extrusion”, Journal of Materials Processing Technology, Vol. 168, pp. 137-146.

6. RESPONSIBILITY NOTICE

The author(s) is (are) the only responsible for the printed material included in this paper.